PROCEEDINGS OF SCIENCE

The Reverberation of UHECR from Local Structure

A. M. Taylor,[a,*] **J. H. Matthews**[b,c] **and A. R. Bell**[d,e]

[a] *Deutsches Elektronen-Synchrotron, Platanenallee 6, 15738 Zeuthen, Germany*
[b] *Department of Physics, Astrophysics, University of Oxford, Denys Wilkinson Building, Keble Road, Oxford, OX1 3RH, UK*
[c] *Institute of Astronomy, University of Cambridge, Madingley Road, Cambridge, CB3 0HA, UK*
[d] *University of Oxford, Clarendon Laboratory, Parks Road, Oxford, OX1 3PU, UK*
[e] *Central Laser Facility, STFC Rutherford Appleton Laboratory, Harwell, Oxford, OX11 0QX, UK*

E-mail: andrew.taylor@desy.de

Observations by the PAO indicate a correlation between UHECRs and either the local AGN or starburst galaxies. We consider whether this correlation is compatible with UHECRs having a single local extragalactic origin, and subsequently ballistically propagating in local extragalactic space before reverberating off the local Council of Giants structure. Focusing effects within the reverberation wave structure observed are discussed. We demonstrate that such a scenario imprints itself on the UHECR skymap, composed of both the direct and secondary waves from both the primary source local and the Council of Giant structure, respectively.

38th International Cosmic Ray Conference (ICRC2023)
26 July - 3 August, 2023
Nagoya, Japan

*Speaker

© Copyright owned by the author(s) under the terms of the Creative Commons Attribution-NonCommercial-NoDerivatives 4.0 International License (CC BY-NC-ND 4.0).

PoS(ICRC2023)215

1. Introduction

The origin if the highest energy cosmic rays drives observational and theoretical studies in high energy astrophysics. Clues to this origin may finally be emerging thanks to deep observations made by the PAO, revealing evidence for small scale anisotropy in the skymaps of these highest energy particles. In particular, these small scale anisotropies appear to correlate with the location in the sky of the most local extragalactic structure [1].

Theoretical motivations for candidate sources can be made through the consideration of both the Hillas [2] and the Hillas-Lovelace criteria [3–6].

The existence of a correlation of UHECR with local extragalactic structure, motivates the consideration of scenarios in which a local AGN, namely Cen A, is the dominant source of UHECR driving the anisotropy signal detected by the PAO [7]. We here further explore this possibility.

The full publication, describing this research in more detail, can be found in [8].

2. The Local Extragalactic Region

The Universe of local extragalactic scales ($\lesssim$ 100 Mpc), is inhomogeneous. Focusing on the local patch of the Universe where the Milky Way resides, substructure is noticed. Specifically, on very local distances $\lesssim$ 10 Mpc around the MW, in a region with distinct kinematics known as the Local Sheet [9]. The most massive galaxies in this region form a ring approximately surrounding the Local Group, and are described as the "Council of Giants" (CoG) by [10]; we adopt this CoG naming convention hereafter.

Within the CoG group member set, only Cen A is recognised to demonstrate clear recent AGN activity required to enable particle acceleration up to the UHECR energy scale. Definitive evidence for this activity in Cen A is revealed by the radio emission detected from its two giant lobe structures, which each extend out to $\approx$ 300 kpc, a distance scale comparable to the virial radius of its host galaxy [11]. In addition to this it also possesses smaller scale inner lobes, indicating the onset of more recent AGN activity [12]. Amongst the CoG members, no other objects display such prominent AGN jet activity.

The thermal and magnetic pressures within the CoG system, outside of the central galaxy environments, remains to be strongly constrained. Recent observations, however, do suggest that a significant amount of thermal pressure of galaxies resides out to virial radii distances ($\sim$ 300 kpc) [13], with hints that magnetic fields at these large radii may also be large [14].

3. Simulation

To simulate the propagation of cosmic rays from Cen A through the COG structure to Earth a Monte Carlo description utilising 1.5×10^9 particles is adopted. The first particles launched at $t = 0$ such that the first particles arrive at Earth after $\approx$ 12 Myr. An isotropic distribution of initial particle momenta is adopted, motivated by the expectation that the particle Larmor radii are small compared to the dimensions of the jet dimensions on these spatial scales.

PoS(ICRC2023)215

Particles are injected into the system at Cen A with a spectral energy distribution of the form

$$\frac{dN}{dE} = \sum_{i=1}^{i_{\max}} f_i \left(\frac{E}{E_0}\right)^{-2} e^{-E/(Z_i R_{\max})}, \tag{1}$$

where a spectral index of 2 has been adopted, as motivated by Fermi diffusive shock acceleration theory for the case of strong shocks [15]. The terms f_i in the expression above describes the abundance of species of i, and $R_{\max}$ is the maximum rigidity that Cen A is assumed to accelerate particles up to. A value for E_0, the minimum energy scales particles are injected at, of 30 EeV is adopted. This value for E_0 is adopted so as to focus our simulations on the energy scale at which small scale anisotropies are observed in the UHECR skymap data. A two species setup is adopted (ie. $i_{\max} = 2$), consisting of He and Fe nuclei. Abundance ratios for He and Fe injected at the sources of $f_{\rm He} = 0.868$, and $f_{\rm Fe} = 0.132$ are adopted. Our motivation for adopting this He : Fe ratio is to ensure that a comparable level of signal (within a factor of 3) in the Model C skymaps from both the direct and reverberated waves.

For particle propagation within the CoG region, we assume isotropic scattering lengths for cosmic rays in close proximity to the CoG objects. For simplicity we adopt energy independent isotropic scattering lengths for all cosmic ray nuclei in the system, with a scattering length,

$$l_{\rm sc} = \begin{cases} c\tau_{\rm sc}, & \text{if } r \leq r_{\rm sc} \\ \infty, & \text{otherwise} \end{cases} \tag{2}$$

where r is the distance of the cosmic ray from the CoG object, and $r_{\rm sc}$ is the galactic scattering radius for the CoG members (fixed to a size of 300 kpc for all objects). This scattering radius value is close to the expected virial radii for a 10^{12} $M_\odot$ mass galaxy. For our description of the scattering events, we adopt a large angle isotropic scattering description.

We consider 3 different possible source evolution models. These models differ in how both the UHECR source luminosity evolution varies with time, and in the UHECR escape time from the source region. We label these models A, B and C. The underlying idea here is that model A provides insight into the response fucntion that the CoG structure imposes on an UHECR pulse from the source. In contrast, models B and C, considred as more plausible scenarios, explore the effect of the source luminosity and escape rate evolution, respectively. Further details of the two scenarios are given below.

For **Model B** we consider a scenario in which the UHECR source luminosity decreases exponentially over time, after the initial injection pulse. For this model, once injected by the source, the particles escape immediately fron the source region. Using the timescale from the initial injection, the subsequent UHECR luminosity is given by,

$$L = L_0 e^{-t/\tau_{\rm dec}}, \ (\text{for } t > 0) \tag{3}$$

where $\tau_{\rm dec}$ describes the decay time of the UHECR source luminosity (set to 3 Myr). This short activity timescale is noted to be consistent with the activity evolution of other local AGN [16].

For **Model C** we consider a scenario in which the source injects a pulse of particles, with these particles subsequently residing for longer within the source region before escaping. We approximate

PoS(ICRC2023)215

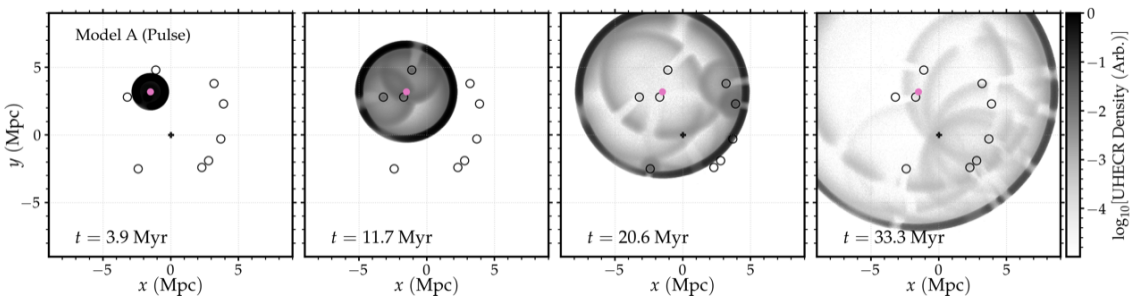

Figure 1: Particle position maps from a slice of thickness $\Delta z = 0.6$ Mpc in the $z = 0$ plane from Model A at four timesteps (3.9 Myr, 11.7 Myr, 20.6 Myr, 33.3 Myr), following their impulsive release from Cen A.

the physics of diffusive escape out of the magnetised lobes by assuming rigidity-dependent particle escape times, given by

$$\tau_{\rm esc} = \tau_{10} \left(\frac{E/Z}{10\ {\rm EV}} \right)^{-1}, \tag{4}$$

where E is the particle energy, Z the particle charge, and τ_{10} is the escape time for a 10 EV rigidity particle, for which we choose $\tau_{10} = 1.5$ Myr. Such an escape time for particles with rigidity 10 EV is consistent with these particles experiencing around 1 scattering event before being able to escape from their source region into the CoG environment.

4. Results

After their propagation through the CoG system, UHECR nuclei arrive to the MW in multiple waves. Fig.1 shows a $z = 0$, $\Delta z = 0.6$ Mpc slice of the arriving particle spatial distribution in the system for Model A at four key timescales: 0 Myr, 12 Myr, 21 Myr, and 33 Myr, in the $x - y$ (local sheet) plane. Also shown in this figure are the positions of the CoG objects (empty circles), Cen A (pink filled circle), and the MW location (black vertical cross). The arrival of waves of particles to the MW location are observed in these particle density plots at 12 Myr, 21 Myr, and 33 Myr.

An understanding of the timescales for which the waves arrive to the MW, and the specific sources responsible at each of these times for contributing to the reverberation signal, can be understood from Fig. 2. This figure gives a breakdown of the reverberated waves, connecting each arrival time to sources located on a specific concentric ellipse, whose two focii are occupied by Cen A and the MW. The colour scale in the figure indicates the delay time for trajectories reverberating off each concentric ellipse.

Plots showing the angular distribution of particles arriving to a MW based observer (i.e. the arriving particle skymap), after scattering off the CoG objects, is shown in Galactic coordinates in Fig. 3 for the model A scenario. This figure shows the arriving cosmic ray skymaps at 33.3 Myr after a Cen A outburst of UHECR. To produce this skymap, we binned the arrival directions into solid angle bins, in Galactic coordinates, using the Healpy python implementation [17] of the HEALpix scheme [18]. The colour-scale in these skymaps encodes the number of particles per pixel (ie. solid angle bin).

Corresponding plots are shown in Fig.s 4 and 5 for model B and C scenarios, respectively. In our framework, and as also suggested by [7], we consider the 33 Myr time period to approximate

PoS(ICRC2023)215

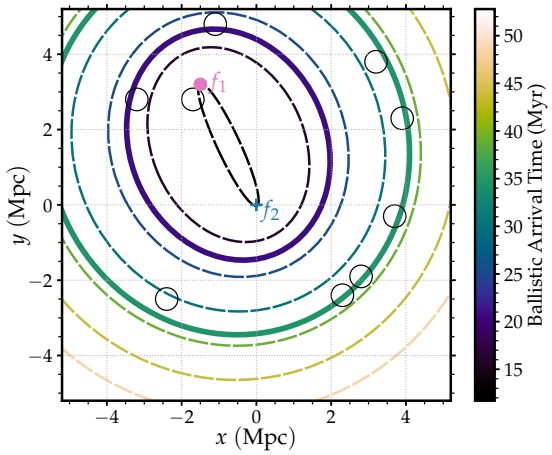

Figure 2: A family of concentric ellipses with a variety of eccentricity values, colour-coded by the corresponding ballistic arrival time to the MW from Cen A. The ellipses are plotted as dashed lines from 11.7 to 52.8 Myr at 2.94 Myr intervals. Additional thick solid lines are overlaid for key timescales of t = 20.6 Myr and t = 33.3 Myr (see also Fig. **??**).

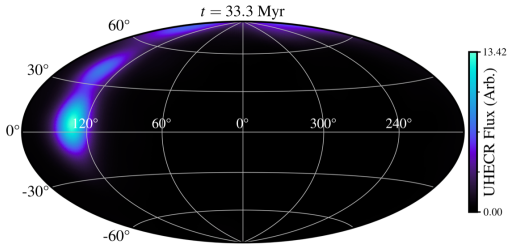

Figure 3: Skymap in Galactic coordinates (Hammer-Aitoff projection) from Model A at 11.7 Myr (top), 20.6 Myr (middle), and 33.3 Myr (bottom) after the impulsive cosmic ray release from Cen A. The colour-scale encodes the number of particles per HEALpix pixel, initially calculated with 32×32 pixels covering the sky, which has then been smoothed with a Gaussian symmetric beam with full-width at half-maximum of 20°. Animations of all skymaps are available in an online repository (see *Data Availability*).

to the present day, representing a reasonable characteristic elapsed time since Cen A's UHECR activity was at its peak. The arriving UHECR flux at these late times (33 Myr) allows for bright spots of comparable intensity in the skymap for both directions towards Cen A, and towards the CoG members located furthest from Cen A. Both the model B and model C skymaps are noted to show striking similarities with the observational results from both the PAO and TA [19–21], in particular when compared to the all-sky anisotropy patterns [22, 23]. Specifically, a hotspot from the direction of Cen A is observed, with additional hotspots being produced by the reverberated signal from the directions of Maffei/IC 342, M81/M82, M94 and M64. It should be highlighted that the relative brightness of the Cen A signal and the reverberation signals depends on the model parameters – specifically the adopted composition, the source activity ($\tau_{\rm dec}$), the CR escape time ($\tau_{\rm esc}$), and the halo size $r_{\rm sc}$. Different relative intensities and extensions can therefore be achieved by tuning these parameters accordingly.

PoS(ICRC2023)215

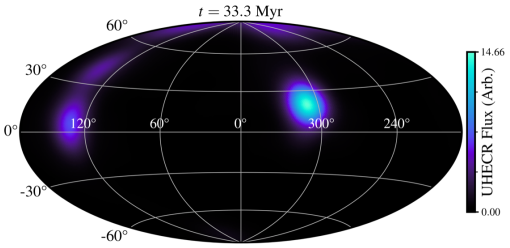

Figure 4: Skymap in Galactic coordinates (Hammer-Aitoff projection) at 33.3 Myr, for Model B, the declining source scenario, for which a decay time of $\tau_{\rm dec} = 3$ Myr has been adopted. The map is calculated in the same way as in Fig. 4.

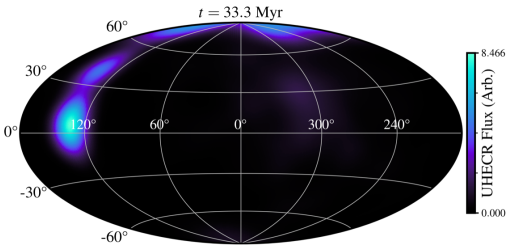

Figure 5: As Fig. 4, but for Model C, the delayed escape scenario in which particles have a rigidity-dependent escape time described by equation 4 with $\tau_{10} = 1.5$ Myr.

5. Conclusions

We consider a local origin for the observed correlation of UHECR with nearby extragalactic structures reported by PAO above an energy of 40 EeV [20, 21] and TA above an energy of 50 EeV [19]. Whether such a UHECR correlation can result from the reverberation signal of UHECR, originally accelerated and released by Cen A, off the local extragalactic structure, developing further a scenario initially considered by [7], is investigated.

Focussing on the effects that the presence of the local CoG (< 10 Mpc) structure might have, we simulate the ballistic propagation of UHECR originating from Cen A, incorporating large angle scattering of the UHECR in close proximity (<300 kpc) to any of the member objects. Our primary finding is that a pulse of UHECR from Cen A, subsequently propagated through the CoG structure, gives rise to three distinct signals. The first wave at 12 Myr, is produced by direct (unhindered) particle propagation from Cen A. The second and third signals, at 21 Myr and 33 Myr, are produced by the reverberation waves from the presence of the local structure.

Additionally we consider the effect introduced on top of these results by both Cen A's source activity evolution over the last 30 Myr (model B), as well as the rigidity dependent escape of UHECR from Cen A (model C). For both of these cases, we show that hotspots are produced in the skymap by the presence of the CoG members (see Fig.s 4 and 5).

PoS(ICRC2023)215

References

[1] A. van Vliet, A. Palladino, A. Taylor and W. Winter, *Extragalactic magnetic field constraints from ultrahigh-energy cosmic rays from local galaxies*, *Monthly Notices of the Royal Astronomical Society* **510** (2022) 1289.

[2] A.M. Hillas, *The Origin of Ultra-High-Energy Cosmic Rays*, *Annual Review of Astronomy and Astrophysics* **22** (1984) 425.

[3] R.V.E. Lovelace, *Dynamo model of double radio sources*, *Nature* **262** (1976) 649.

[4] E. Waxman, *High-energy cosmic rays: Puzzles, models and giga-ton neutrino telescopes*, *Pramana* **62** (2004) 483 [astro-ph/0310079].

[5] C.A. Norman, D.B. Melrose and A. Achterberg, *The Origin of Cosmic Rays above 10 18.5 eV*, *The Astrophysical Journal* **454** (1995) 60.

[6] R.D. Blandford, *Acceleration of Ultra High Energy Cosmic Rays*, *Physica Scripta Volume T* **85** (2000) 191.

[7] A.R. Bell and J.H. Matthews, *Echoes of the past: ultra-high-energy cosmic rays accelerated by radio galaxies, scattered by starburst galaxies*, *Monthly Notices of the Royal Astronomical Society* **511** (2022) 448.

[8] A.M. Taylor, J.H. Matthews and A.R. Bell, *UHECR Echoes from the Council of Giants*, 2302.06489.

[9] R.B. Tully, E.J. Shaya, I.D. Karachentsev, H.M. Courtois, D.D. Kocevski, L. Rizzi et al., *Our Peculiar Motion Away from the Local Void*, *The Astrophysical Journal* **676** (2008) 184.

[10] M.L. McCall, *A Council of Giants*, *Monthly Notices of the Royal Astronomical Society* **440** (2014) 405.

[11] K.V. Sheridan, *An investigation of the strong radio sources in Centaurus, Fornax and Puppis.*, *Australian Journal of Physics* **11** (1958) 400.

[12] J.H. Croston, R.P. Kraft, M.J. Hardcastle, M. Birkinshaw, D.M. Worrall, P.E.J. Nulsen et al., *High-energy particle acceleration at the radio-lobe shock of Centaurus A*, *Monthly Notices of the Royal Astronomical Society* **395** (2009) 1999 [0901.1346].

[13] J.N. Bregman, E. Hodges-Kluck, Z. Qu, C. Pratt, J.-T. Li and Y. Yun, *Hot Extended Galaxy Halos around Local L* Galaxies from Sunyaev–Zeldovich Measurements*, *Astrophys. J.* **928** (2022) 14 [2107.14281].

[14] V. Heesen, S.P. O'Sullivan, M. Brüggen, A. Basu, R. Beck, A. Seta et al., *Detection of magnetic fields in the circumgalactic medium of nearby galaxies using Faraday rotation*, *arXiv e-prints* (2023) arXiv:2302.06617 [2302.06617].

PoS(ICRC2023)215

[15] F.C. Jones, *A Theoretical Review of Diffusive Shock Acceleration*, *Astrophysical Journal Supplement Series* **90** (1994) 561.

[16] D.J. Saikia and M. Jamrozy, *Recurrent activity in Active Galactic Nuclei*, *Bulletin of the Astronomical Society of India* **37** (2009) 63 [1002.1841].

[17] A. Zonca, L. Singer, D. Lenz, M. Reinecke, C. Rosset, E. Hivon et al., *healpy: equal area pixelization and spherical harmonics transforms for data on the sphere in Python*, *The Journal of Open Source Software* **4** (2019) 1298.

[18] K.M. Górski, E. Hivon, A.J. Banday, B.D. Wandelt, F.K. Hansen, M. Reinecke et al., *HEALPix: A Framework for High-Resolution Discretization and Fast Analysis of Data Distributed on the Sphere*, *The Astrophysical Journal* **622** (2005) 759.

[19] Telescope Array collaboration, *Indications of Intermediate-Scale Anisotropy of Cosmic Rays with Energy Greater Than 57 EeV in the Northern Sky Measured with the Surface Detector of the Telescope Array Experiment*, *Astrophys. J. Lett.* **790** (2014) L21 [1404.5890].

[20] A. Aab, P. Abreu, M. Aglietta, I.F.M. Albuquerque, I. Allekotte, A. Almela et al., *An Indication of Anisotropy in Arrival Directions of Ultra-high-energy Cosmic Rays through Comparison to the Flux Pattern of Extragalactic Gamma-Ray Sources*, *Astrophys. J. Lett.* **853** (2018) L29 [1801.06160].

[21] Pierre Auger collaboration, *Arrival Directions of Cosmic Rays above 32 EeV from Phase One of the Pierre Auger Observatory*, *Astrophys. J.* **935** (2022) 170 [2206.13492].

[22] J. Biteau, T. Bister, L. Caccianiga, O. Deligny, A. di Matteo, T. Fujii et al., *Covering the celestial sphere at ultra-high energies: Full-sky cosmic-ray maps beyond the ankle and the flux suppression*, in *European Physical Journal Web of Conferences*, vol. 210 of *European Physical Journal Web of Conferences*, p. 01005, Oct., 2019, DOI [1905.04188].

[23] A. di Matteo, T. Bister, J. Biteau, L. Caccianiga, O. Deligny, T. Fujii et al., *Full-sky searches for anisotropies in UHECR arrival directions with the Pierre Auger Observatory and the Telescope Array*, *arXiv e-prints* (2020) arXiv:2001.01864 [2001.01864].

PoS(ICRC2023)215